HYPOELLIPTIC DIFFUSION AND HUMAN VISION

Ugo Boscain
CNRS, CMAP, École Polytechnique, Route de Saclay, 91128 Palaiseau Cedex, France
and INRIA Team GECO, boscain@cmap.polytechnique.fr

Jean-Paul Gauthier
LSIS, UMR CNRS 7296, Universté de Toulon USTV, 83957, La Garde Cedex, France
and INRIA Team GECO, gauthier@univ-tln.fr

Roman Chertovskih
Centre for Wind Energy and Atmospheric Flows, Faculdade de Engenharia da Universidade do Porto, Rua Dr. Roberto Frias s/n, 4200-465 Porto, Portugal
and International Institute of Earthquake Prediction Theory and Mathematical Geophysics, Profsoyuznaya str. 84/32, 117997 Moscow, Russia, roman@mitp.ru

Alexey Remizov
CMAP, École Polytechnique CNRS, Route de Saclay, 91128 Palaiseau Cedex, France, alexey-remizov@yandex.ru

Abstract. This paper is devoted to the validation of the theory of neurogeometry of vision, due to Jean Petitot. We focus on the theoretical and numerical aspects of integration of a certain hypoelliptic diffusion operator that appears in the theory. We provide, at the end, a complete numerical algorithm, fully parallellizable.

Subjclass: Primary 94A08; Secondary 35H10, 93C10, 93C20
Keywords: sub-Riemannian geometry, image reconstruction, hypoelliptic diffusion

1. Introduction

In his beautiful book [30], Jean Petitot proposes a sub-Riemannian theory for the neurogeometry of (human) vision; see also [10]. For mathematical aspects we refer also to our previous paper [6]. The main idea goes back to the 1981 Nobel prize of Hübel an Wiesel, who showed that in the human visual cortex V1, there are groups of Neurons that are sensitive to position, and groups of Neurons that are sensitive to direction, with connections between them that are activated by the image.

So that it is presumable that V1 in fact lifts the images $f(x, y)$ (that are functions of two position variables x, y in the plane $\mathbb{R}^2$ of the image) to functions over the projective tangent bundle $PT\mathbb{R}^2$. This bundle $PT\mathbb{R}^2$ has a contact structure which is invariant under the action of the group $SE(2)$ of motions of the plane, that will be described precisely just below, and that is denoted by $\blacktriangle$ in vector distribution form.

Then, Jean Petitot was naturally led to consider sub-Riemannian structures over $PT\mathbb{R}^2$ also invariant under the action of $SE(2)$, i.e., motion-invariant Riemannian metrics over ▲.

Since we will be obliged at some point to go to certain stochastic considerations, it is convenient to consider the following sub-Riemannian structure in a "control system form"

$$\begin{pmatrix} \dot{x} \\ \dot{y} \\ \dot{\theta} \end{pmatrix} = u \begin{pmatrix} \cos(\theta) \\ \sin(\theta) \\ 0 \end{pmatrix} + v \begin{pmatrix} 0 \\ 0 \\ 1 \end{pmatrix} = uF + vG, \tag{1.1}$$

where (x, y, θ) are the coordinates on $PT\mathbb{R}^2$; u, v are the controls; F, G are vector fields given by the formulae

$$F = \cos(\theta)\frac{\partial}{\partial x} + \sin(\theta)\frac{\partial}{\partial y}, \quad G = \frac{\partial}{\partial \theta}. \tag{1.2}$$

The distribution ▲ is generated by the vector fields F, G defined in (1.2). Since $\dim ▲ = 2$ and the Hörmander condition[1] holds true at any point, ▲ defines a sub-Riemanninan structure on the bundle $PT\mathbb{R}^2$. The Riemannian metric $\langle \cdot, \cdot \rangle$ is specified via the "controls" u, v, by the fact that F, G form an orthonormal frame field.

The length of an admissible (i.e., everywhere tangent to ▲) smooth curve Γ, $\Gamma(t) = (x(t), y(t), \theta(t))$, is therefore $L(\Gamma) = \int_\Gamma \sqrt{\dot{x}^2 + \dot{y}^2 + \dot{\theta}^2}\, dt$. The sub-Riemanninan distance between two points of $PT\mathbb{R}^2$ is the minimum length of admissible curves connecting these points.

In practice, it appears important to introduce a weight parameter $\alpha > 0$ and the corresponding metric $L_\alpha(\Gamma) = \int_\Gamma \sqrt{\dot{x}^2 + \dot{y}^2 + \alpha\dot{\theta}^2}\, dt$. The meaning of the parameter α will be discussed later (section 2.3.1).

Remark 1. *1. The formula* (1.1) *is not global over $PT\mathbb{R}^2$: this sub-Riemannian structure is not trivializable. However, if we lift it to the group $SE(2)$, which is a double covering of $PT\mathbb{R}^2$, it becomes trivializable and the equation* (1.1) *becomes global.*

2. It was noticed by A. Agrachev that this is the only sub-Riemannian structure over $PT\mathbb{R}^2$ which is invariant under the action of $SE(2)$.

3. From the theoretical point of view, the weight parameter α is irrelevant: for any $\alpha > 0$ there exists a homothety of the (x, y)-plane that maps geodesics of the metric with the weight parameter α to those of the metric with $\alpha = 1$.

For the same reasons as in Riemannian geometry, minimizing the length $L(\Gamma)$ is the same as minimizing the energy $E(\Gamma) = \int_\Gamma (\dot{x}^2 + \dot{y}^2 + \dot{\theta}^2)\, dt = \int_\Gamma u^2(t)dt + \int_\Gamma v^2(t)\, dt$. From the vision point of view, the term $\int_\Gamma u^2(t)\, dt$ is the energy necessary to activate neurons that are sensitive to position in the plane, while $\int_\Gamma v^2(t)\, dt$ is the energy necessary to activate neurons that are sensitive to direction.

The idea is that, **when reconstructing a corrupted image**, the visual cortex V1 will minimize the energy necessary to activate the neurons that are not activated, in the corrupted part of the image. For this, consider an individual interrupted level curve $f(x, y) = \text{const}$. It is reasonable to complete it by a geodesic of the

[1]The Hörmander condition reads: $\text{span}\{F, G, [F, G]\} = T_q PT\mathbb{R}^2$ for any $q \in PT\mathbb{R}^2$.

sub-Riemannian structure, that minimizes energy of neurons to be activated. In this direction, behind an important theoretical contribution, successful practical results were obtained [31, 32]. However, for a corrupted piece of a real image, it is not clear how to put in correspondence the non-corrupted parts of the same level set.

For that reason, to reconstruct a corrupted image (the V1 inpainting problem), it is natural to proceed as follows: in system (1.1), excite all possible admissible paths in a stochastic way. One gets a stochastic differential equation

$$\begin{pmatrix} dx_t \\ dy_t \\ d\theta_t \end{pmatrix} = \begin{pmatrix} \cos(\theta_t) \\ \sin(\theta_t) \\ 0 \end{pmatrix} du_t + \begin{pmatrix} 0 \\ 0 \\ 1 \end{pmatrix} dv_t, \tag{1.3}$$

where u_t, v_t are two independent Wiener processes.

Consider the associated diffusion process:

$$\frac{\partial \psi}{\partial t} = \frac{1}{2}\Delta\psi, \quad \Delta = F^2 + G^2 = \left(\cos(\theta)\frac{\partial}{\partial x} + \sin(\theta)\frac{\partial}{\partial y}\right)^2 + \frac{\partial^2}{\partial \theta^2}. \tag{1.4}$$

The operator Δ is hypoelliptic (satisfies Hörmander condition). By the Feynman–Kac formula, integrating Equation (1.4) with the corrupted image as the initial condition, **one expects to reconstruct the most probable missing level curves** (among admissible).

To summarize, the analysis of Jean Petitot of the process of reconstruction by V1 of corrupted images is the following (we refer to [6] for details):

- The plane image $f(x, y)$ is lifted to a certain "function" $\overline{f}(x, y, \theta)$ on the bundle $PT\mathbb{R}^2$.
- The diffusion process (1.4) with the initial condition $\psi\big|_{t=0} = \overline{f}$ is integrated on the interval $t \in [0, T]$ for some $T > 0$.
- The resulting function $\overline{f}_T = \psi\big|_{t=T}$ on the bundle $PT\mathbb{R}^2$ is projected down to a function $f_T(x, y)$, which represents the reconstructed image.

The lifting procedure should be as follows: the image is assumed to be a smooth[2] function $f(x, y)$. Then, it can be naturally lifted to a surface S in $PT\mathbb{R}^2$ by lifting its level curves. At a point (x, y, θ) we would like to set $\overline{f}(x, y, \theta) = f(x, y)$ if $(x, y, \theta) \in S$ and $\overline{f}(x, y, \theta) = 0$ elsewhere. But this would be nonsense since S has zero measure in $PT\mathbb{R}^2$. Hence in the Petitot model $f(x, y)$ is lifted to a distribution $\overline{f}(x, y, \theta)$, supported in S, and weighted by $f(x, y)$.

It turns out that although looking rather simple, Equation (1.4) is not that easy to integrate. In particular, the multiscale sub-Riemannian effects are hidden inside. We refer to our previous paper [2] for the computation of the associated heat kernel, but the direct use of the kernel appears quickly not very tractable. Moreover, the numerical integration starts to be a quite large problem, due to the number of points/angles in a reasonable image. To get an idea of the size of the full space-discretization of the problem, see Remark 4 below.

Hence a significant part of the paper is devoted to the numerical integration of this equation.

[2] In fact, it is known by biologists that a certain smoothing procedure is already applied at the level of the retina [12, 25, 28].

It turns out that we were led to rather abstract considerations, to get at the end a quite simple algorithm, massively parallelizable. This aspect of parallelizability seems to fit with the structure of the visual cortex V1, which is suspected, due to this structure, to make a lot of parallel computations.

The paper is organized as follows: in the next section 2, we discuss some properties of the group $SE(2)$ and its discrete avatars, together with a discrete version of the hypoelliptic diffusion (1.4).

Section 3 presents our main ideas and shows a first algorithm, which is not suitable in our case, mostly for two reasons:

- The "distributional" nature of lifted images (initial conditions).
- Compared to our final algorithm, it does not present the capability to treat in a different way the corrupted and non-corrupted parts of the image (see Section 5).

However, this approach could certainly be interesting for more smooth initial conditions.

Section 4 presents our final algorithm which, due to the abstract structure of the groups under consideration, is massively parallel: It reduces the problem to a number of problems of integration of linear differential equations in low dimension, completely decoupled.

Section 5 presents a heuristic improvement of the algorithm in the case where we can distinguish between the corrupted and non-corrupted parts of the image.

Finally, a very short appendix is devoted to basic theoretical concepts and to certain technical computations.

We do not pretend that our results are better than the inpainting algorithms existing to day. We just claim that they really seem to validate the theory of Jean Petitot and we emphasize the global character of the algorithm.

We do not discuss the final step of the algorithm (projection) here. There are at least two obvious possibilities: projecting by taking either the maximum, or the average, over angles. Numerous experiments show that the projection made by the maximum provides better results.

2. The Operators and the groups under consideration

2.1. **Groups.** We advise the uninitiated reader to start with our paper [2] and to have a look to the appendix at the end of this paper.

2.1.1. *The group of Motions SE(2).* The group law over the Lie group $SE(2)$ has multiplication law $(X_2, \theta_2) \cdot (X_1, \theta_1) = (X_2 + R_{\theta_2} X_1, \theta_1 + \theta_2)$, where

$$X = \begin{pmatrix} x \\ y \end{pmatrix}, \quad R_\theta = \begin{pmatrix} \cos(\theta) & \sin(\theta) \\ -\sin(\theta) & \cos(\theta) \end{pmatrix},$$

R_θ is the rotation of angle θ in the X-plane.

The (strongly continuous) unitary irreducible representations of $SE(2)$ are well known. However for analogy with the next section, we need to recall basic facts. For a survey, see [34, 35].

As representations of a semi-direct product, they can be obtained by using Mackey's imprimitivity theorem, and therefore, they are parametrized by the orbits of the (contragredient) action of rotations on the X-plane, i.e., they are parametrized by the half lines passing through the origin. Additionally, corresponding to the origin, there are the characters of the rotation group S^1 that do not count in the

support of the Plancherel's measure. Finally, the representation χ_λ corresponding to the circle of radius λ acts over $L^2(S^1)$, and is given by

$$[\chi_\lambda(X,\theta)\cdot\varphi](u) = e^{i\langle v_\lambda, R_u X\rangle}\varphi(u+\theta),$$

where v_λ is a vector of length λ in $\mathbb{R}^2$ and $\langle\cdot,\cdot\rangle$ denotes the standard Euclidean scalar product over $\mathbb{R}^2$.

Note that $SE(2)$ is far from being maximally almost periodic, since all its finite dimensional unitary irreducible representations are given by the characters of S^1 only.

Let us also recall [2, 6, 13, 14] that our sub-Riemannian heat kernel corresponding to the hypoelliptic Laplacian $\frac{1}{2}\Delta$ defined in (1.4) is given by

$$P_t(X,\theta) = \frac{1}{2}\int_0^{+\infty}\left(\sum_{n=0}^{+\infty} e^{a_n^\lambda t}\left\langle \mathrm{ce}_n\left(\theta,\frac{\lambda^2}{4}\right),\, \chi_\lambda(X,\theta)\,\mathrm{ce}_n\left(\theta,\frac{\lambda^2}{4}\right)\right\rangle + \sum_{n=0}^{+\infty} e^{b_n^\lambda t}\left\langle \mathrm{se}_n\left(\theta,\frac{\lambda^2}{4}\right),\, \chi_\lambda(X,\theta)\,\mathrm{se}_n\left(\theta,\frac{\lambda^2}{4}\right)\right\rangle \lambda d\lambda, \tag{2.1}$$

where the functions se_n and ce_n are the 2π-periodic Mathieu sines and cosines, and $a_n^\lambda = -\frac{\lambda^2}{4} - a_n\big(\frac{\lambda^2}{4}\big)$, $b_n^\lambda = -\frac{\lambda^2}{4} - b_n\big(\frac{\lambda^2}{4}\big)$, with a_n, b_n, the characteristic values for the Mathieu equation.

Then the solution of the diffusion equation (1.4) with the initial condition $\psi\big|_{t=0}=\psi_0$ is given by the right-convolution formula:

$$\psi(t,X,\theta) = e^{t\Delta}\psi_0(X,\theta) = \psi_0(X,\theta) * P_t(X,\theta) = \int_{SE(2)} \psi_0(g) P_t\big(g^{-1}\cdot(X,\theta)\big)\, dg, \tag{2.2}$$

where $g \in SE(2)$ and dg is the Haar measure: $dg = dxdyd\theta$. Unfortunately, in practice formula (2.2) is not very tractable, for several reasons (in particular, due to the slow convergence and the difficulty to find good computer implementations of Mathieu functions).

2.1.2. *The group of discrete motions $SE(2,N)$.* In the next section, a discrete-angle version of the above diffusion equation will appear naturally. It corresponds to the group of motions $SE(2)$ restricted to rotations with angles $\frac{2k\pi}{N}$. This group is denoted by $SE(2,N)$. It has very special features: it is maximally almost periodic, and all its unitary irreducible representations are finite dimensional (it is a Moore group, see [20] for details), although it is not compact. This follows in particular from [16, 16.5.3, page 304]: it is the semi-direct product of a compact subgroup $K = \mathbb{Z}/N\mathbb{Z}$, and a normal subgroup V isomorphic to $\mathbb{R}^2$, each element of V commuting with the connected component of the identity (which in this case is V itself). To simplify, we set $R_k = R_{\frac{2k\pi}{N}}$.

Besides the characters of K, the representations coming in the support of the Plancherel measure are parametrized by $(\lambda,\nu) \in \mathbb{R}_*^+ \times [0, \frac{2\pi}{N}[= \widehat{SE(2,N)}$, the **dual**[3] of $SE(2,N)$. They act on $\mathbb{C}^N$ and are given by

$$\chi_{\lambda,\nu}(X,r) = \mathrm{diag}_k\big(e^{i\langle V_{\lambda,\nu}, R_k X\rangle}\big) S^r, \tag{2.3}$$

[3] The natural "dual topology" of $\widehat{SE(2,N)}$ is that of a cone, that consists of considering $\mathbb{R}_*^+ \times [0, \frac{2\pi}{N}]$ and identifying $(\lambda, 0)$ with $(\lambda, \frac{2\pi}{N})$.

where $\mathrm{diag}_k\big(e^{i\langle V_{\lambda,\nu},R_kX\rangle}\big)$ is the diagonal matrix with diagonal elements $e^{i\langle V_{\lambda,\nu},R_kX\rangle}$, $V_{\lambda,\nu}=(\lambda\cos(\nu),\lambda\sin(\nu))$, $k=1,\dots,N$, and S is the shift matrix over $\mathbb{C}^N$ (i.e., $Se_k=e_{k+1}$ for $k=1,\dots,N-1$, and $Se_N=e_1$).

2.2. **The semi-discrete diffusion operator.**

2.2.1. *Semi-discrete versus continuous.* Firstly, we show that a certain semi-discrete (discretization with respect to the angle) model of the diffusion is compatible with the limit continuous model. For the considerations in this section, one may refer to the paper [4].

The diffusion equation (1.4) comes from the stochastic differential equation (1.3), where u_t, v_t are two independent standard Wiener processes. The diffusion equation (1.4) is the associated Fokker-Planck (or Kolmogorov forward) equation for (1.3).

From the image processing point of view, integrating the diffusion is equivalent to excite all possible admissible paths, in a stochastic way. In fact, **in the real structure of the V1 cortex, not all angles are represented**, but a small number only. This number is denoted by N.

Therefore, it is natural to consider the following stochastic process with jumps evidently connected with the stochastic equation (1.3):

$$dz_t=\begin{pmatrix}dx_t\\ dy_t\end{pmatrix}=\begin{pmatrix}\cos(\theta_t)\\ \sin(\theta_t)\end{pmatrix}dv_t, \tag{2.4}$$

in which θ_t is a jump process. Set $\Lambda_N=(\lambda_{i,j})$, $i,j=0,\dots,N-1$, where

$$\lambda_{i,j}=\lim_{t\to 0}\frac{\mathsf{P}\left[\theta_t=e_j|\theta_0=e_i\right]}{t}\quad\text{for}\quad i\neq j,\quad \lambda_{j,j}=-\sum_{i\neq j}\lambda_{i,j}.$$

The matrix Λ_N is the infinitesimal generator of the jump process.

We assume Markov processes, where the law of the first jump time is exponential, with parameter $\beta>0$ (that will be specified later on). The jump has probability $\frac{1}{2}$ on both sides. Then we get a Poisson process, and the probability of k jumps between 0 and t is

$$\mathsf{P}\left[k\text{ jumps}\right]=\frac{(\beta t)^k}{k!}e^{-\beta t}.$$

So that:

$$\begin{aligned}\mathsf{P}\left[\theta_t=e_{i\pm1}|\theta_0=e_i\right]&=\frac{1}{2}\big(\beta t+kt^2+o(t^2)\big)e^{-\beta t},\\ \mathsf{P}\left[\theta_t=e_{i\pm2}|\theta_0=e_i\right]&=\frac{1}{4}\left(\frac{1}{2}\beta^2t^2+o(t^2)\right)e^{-\beta t},\\ \mathsf{P}\left[\theta_t=e_{i\pm n}|\theta_0=e_i\right]&=O(t^n)e^{-\beta t},\quad n=2,3,\dots,\end{aligned}$$

with the convention that e_i is modulo N.

Hence $\lambda_{i,i\pm1}=\frac{1}{2}\beta$ and $\lambda_{i,i}=-\beta$. All other elements of the matrix Λ_N are equal to zero. Then, the infinitesimal generator of the semi-group associated with the stochastic process (z_t,θ_t) is of the form:

$$\mathcal{L}_N\Psi(z,e_i)=(A\Psi)_i(z)+(\Lambda_N\Psi(z,e_i))_i, \tag{2.5}$$

where $\Psi_j(z)=\Psi(z,e_j)$, $z=(x,y)$, and

$$(A\Psi)_i(z)=A\Psi(z,e_i)=\frac{1}{2}\left(\cos(e_i)\frac{\partial}{\partial x}+\sin(e_i)\frac{\partial}{\partial y}\right)^2\Psi(z,e_i), \tag{2.6}$$

$$(\Lambda_N\Psi(z,e_i))_i=\sum_{j=0}^{n-1}\lambda_{i,j}\Psi_j(z)=\frac{\beta}{2}\big(\Psi_{i-1}(z)-2\Psi_i(z)+\Psi_{i+1}(z)\big). \tag{2.7}$$

Therefore, if we set $\beta=\left(\frac{N}{2\pi}\right)^2$, we get

$$(\Lambda_N\Psi(z,e_i))_i=\frac{1}{2}\frac{\Psi_{i-1}(z)-2\Psi_i(z)+\Psi_{i+1}(z)}{\left(\frac{2\pi}{N}\right)^2}=\frac{1}{2}\frac{\partial^2}{\partial\theta^2}\Psi(z,e_i)+O\Big(\frac{1}{N}\Big)^2.$$

At the limit $N\to\infty$, from formulae (2.5) – (2.7) we get the second order differential operator

$$\mathcal{L}\Psi(z,\theta)=\frac{1}{2}\bigg(\Big(\cos(\theta)\frac{\partial}{\partial x}+\sin(\theta)\frac{\partial}{\partial y}\Big)^2+\frac{\partial^2}{\partial\theta^2}\bigg)\Psi(z,\theta)=\frac{1}{2}\Delta\Psi(z,\theta),$$

that is, the operator of our diffusion process (1.4). However the exact Fokker-Planck equation[4] with number of angles $N\ll\infty$ contains the parameter β:

$$\begin{aligned}\frac{d\psi_r}{dt}(t,z)=\frac{1}{2}\bigg(\cos(e_r)\frac{\partial}{\partial x}+\sin(e_r)\frac{\partial}{\partial y}\bigg)^2\psi_r(t,z)+\\ \frac{\beta}{2}\big(\psi_{r-1}(t,z)-2\psi_r(t,z)+\psi_{r+1}(t,z)\big),\quad r=0,\dots,N-1.\end{aligned} \tag{2.8}$$

2.2.2. *The semi-discrete heat kernel via the GFT.* The GFT (generalized noncommutative Fourier transform, see [2] and Appendix here) transforms our hypoelliptic diffusion equation into a continuous sum of diffusions with elliptic right-hand term, and the summation over $\widehat{SE(2,N)}$ is with respect to the Plancherel measure $\lambda d\lambda d\nu$. We compute the semi-discrete heat kernel via the GFT, just as in [2], and we get a similar but simpler formula than for the "continuous" heat kerne (2.1) in the case of the group $SE(2)$:

Formulae (6.1) and (6.2) for the direct and the inverse GFT show that, if we set

$$\widetilde{A}_{\lambda,\nu}=\Lambda_N-\mathrm{diag}_k\big(\lambda^2\cos^2(e_k-\nu)\big), \tag{2.9}$$

we get the following expression for the "semi-discrete" (or "jump") heat kernel:

$$D_t(z,e_r)=\int\limits_{\widehat{SE(2,N)}}\mathrm{trace}\Big(e^{\widetilde{A}_{\lambda,\nu}t}\cdot\mathrm{diag}_k\Big(e^{i\langle V_{\lambda,\nu},R_kz\rangle}\Big)S^r\Big)\lambda d\lambda d\nu. \tag{2.10}$$

Note also that it is a closed formula similar to the one in the Heisenberg case (explicit usual functions modulo a Fourier transform). These are the only cases we know for noncompact groups, where the kernel is obtained with such a formula.

2.2.3. *A direct way to compute the semi-discrete heat kernel.* We start from our semi-discrete heat equation (2.8). The heat kernel is the convolution kernel associated with $D_t(z,e_r)$, the fundamental solution of Equation (2.8).

Applying the ordinary Fourier Transform with respect to the space variable z to (2.8), we get the ordinary linear differential equation

$$\frac{d}{dt}\widetilde{D}_t(z)=\widetilde{A}_{\lambda,\nu}\widetilde{D}_t(z), \tag{2.11}$$

[4]Note that here, due to self adjointness, the Kolmogorov-backward equation is the same as the Kolmogorov-forward one (Fokker-Planck).

where $\widetilde{D}_t(z) = \big(D_t(z,e_1),\dots,D_t(z,e_N)\big)$, with the initial condition obtained from the Dirac delta function at the identity by the ordinary Fourier Transform:

$$\widetilde{D}_0(z) = \delta_N = (0,\dots,0,1).$$

Then, taking the inverse ordinary Fourier Transform with respect to the space variable, we get a second expression for the heat kernel:

$$D_t(z,e_r) = \int_{\mathbb{R}^2} \Big(e^{\widetilde{A}_{\lambda,\nu}t}\delta_N\Big)_r\, e^{i\langle V_{\lambda,\nu},z\rangle}\lambda d\lambda d\nu, \tag{2.12}$$

where the subscript r means the r-th coordinate of a vector.

Remark 2. *Looking at the formulae* (2.10) *and* (2.12)*, it is not clear that these expressions are identical. The proof of this fact is given in the appendix (section 6.3). Although less direct, we prefer formula* (2.10)*, that reflects more the structure of* $SE(2,N)$*.*

2.3. **Two important points.**

2.3.1. *The weighting of the metric.* Consider the diffusion process

$$\frac{\partial\psi}{\partial t} = \frac{1}{2}\Delta_\alpha\psi, \quad \Delta_\alpha = F^2 + \alpha G^2 = \left(\cos(\theta)\frac{\partial}{\partial x} + \sin(\theta)\frac{\partial}{\partial y}\right)^2 + \alpha\frac{\partial^2}{\partial\theta^2} \tag{2.13}$$

with the weighting coefficient $\alpha > 0$. The hypoelliptic operator Δ defined in (1.4) is the case $\alpha = 1$. Although the coefficient α is theoretically irrelevant (see Remark 1, item 3), it plays an essential role in practice.

On the same way, for the semi-discrete operator, we have

$$\Delta^{(N)}\psi_i(t,z) =$$
$$\left(\cos(e_i)\frac{\partial}{\partial x} + \sin(e_i)\frac{\partial}{\partial y}\right)^2\psi_i(t,z) + \beta\big(\psi_{i-1}(t,z) - 2\psi_i(t,z) + \psi_{i+1}(t,z)\big) =$$
$$\left(\left(\cos(e_i)\frac{\partial}{\partial x} + \sin(e_i)\frac{\partial}{\partial y}\right)^2 + \beta\Big(\frac{2\pi}{N}\Big)^2\frac{\partial^2}{\partial\theta^2}\right)\psi_i(t,z) + O\Big(\frac{1}{N}\Big)^2$$

as $N\to\infty$. Comparing the above formula with (2.8), we have the relation:

$$\alpha = \beta\Big(\frac{2\pi}{N}\Big)^2. \tag{2.14}$$

It appeared clearly in all our experiments that $N = 30$ is always enough (it brings nothing visible in the experiments to take $N > 30$).

Both parameters N and β have a physiological meaning. Therefore, the coefficient α of the limit behavior ($N\to\infty$) can certainly be obtained from physiological considerations.

2.3.2. *The effect of the projectivisation on the kernel.* This is related to the known phenomenon called "chirality of the pinwheels": the pinwheels are cells in some pictures that are obtained by observing cuts of the V1 cortex. They put in evidence the sensitivity of certain neurons to directions, and they show clearly that certain groups of neurons have spatial chirality. This could be reflected in formula (2.15) below.

As we said, the neurons are not sensitive to the angles themselves, but to directions only (i.e., the angles are modulo π and not 2π). It is the reason why we

work in the projectivisation $PT\mathbb{R}^2$ of the tangent bundle of $\mathbb{R}^2$, in place of $SE(2)$ itself. From the discrete point of view, it means that if N is the number of values of directions (not angles), the angle-step is in fact $\frac{\pi}{N}$.

Also, as it was explained in [6], the sub-Riemannian structure over $PT\mathbb{R}^2$ itself is not trivializable. This is not a problem for the operators Δ and $\Delta^{(N)}$, since the functions $\cos(\theta)^2$, $\sin(\theta)^2$ and $\sin(2\theta)$ are π-periodic. **Hence, details relative to this projectivisation are omitted in the following sections**.

From the point of view of the heat kernels, in fact, if p_t denotes the heat kernel over $PT\mathbb{R}^2$ (which is not a group convolution kernel anymore, since $PT\mathbb{R}^2$ is not a group), we have the formula

$$p_t((x,y,\theta),(\bar{x},\bar{y},\bar{\theta})) = P_t((\bar{x},\bar{y},\bar{\theta})^{-1}\cdot(x,y,\theta)) + P_t((\bar{x},\bar{y},\bar{\theta})^{-1}\cdot(x,y,\theta+\pi)), \tag{2.15}$$

where the inverses and products are intended in the group $SE(2)$.

A similar formula holds for the semi-discrete kernels d_t and D_t (from (2.10)) for even N.

3. A pre-algorithm

As we said in section 2.1.2, the group $SE(2,N)$ is maximally almost periodic. It follows from the expression (2.3) of the unitary irreducible representations that the Bohr-almost periodic functions $f(x,y,r)$ are just those such that the functions $f_r(x,y) = f(x,y,r)$, $r = 1,\dots,N$, are Bohr-almost periodic over $\mathbb{R}^2$ in the usual sense. We call $AP(N)$ the set of almost periodic functions on $SE(2,N)$, and we identify the elements of $AP(N)$ to $\mathbb{C}^N$-valued functions whose components are almost periodic over $\mathbb{R}^2$, i.e., functions that are uniform limits of trigonometric polynomials in the two variables (x,y).

These functions are dense among continuous functions over any compact subset of $SE(2,N)$, and $AP(N)$ is a good candidate for the space of solutions of our heat equation: exactly as for the usual heat equation (see [11, pp. 144–146] for instance), the uniformly bounded solutions of our heat equation with initial conditions in $AP(N)$ remain almost periodic over $SE(2,N)$ uniformly in time.

Functions coming from practical images have support in a bounded subset of $SE(2,N)$. They can be (after smoothing and lifting) approximated uniformly over this bounded subset by trigonometric $\mathbb{C}^N$-valued polynomials $Q(x,y)$ with components $Q_r(x,y)$:

$$Q_r(x,y) = \sum_{i=0}^{k} a_{r,\lambda_i,\mu_i} e^{i(\lambda_i x + \mu_i y)}. \tag{3.1}$$

The vector space of such $\mathbb{C}^N$-valued polynomials, for a fixed finite number of distinct values of λ_i, μ_i, i.e., $\omega = (\lambda_i,\mu_i) \in K$, a fixed finite subset of $\mathbb{R}^2$, is denoted by $SE(2,N,K)$.

A trivial computation shows that semi-discrete hypoelliptic equation (2.8) restricts to $SE(2,N,K)$. It becomes

$$\frac{da_r^i}{dt} = -\frac{1}{2}\Big(\lambda_i\cos(\theta_r) + \mu_i\sin(\theta_r)\Big)^2 a_r^i + \frac{\beta}{2}\Big(a_{r+1}^i - 2a_r^i + a_{r-1}^i\Big), \tag{3.2}$$

or, equivalently,

$$\frac{dA^i}{dt} = -\frac{1}{2}\mathrm{diag}_k\big(\lambda_i\cos(\theta_k) + \mu_i\sin(\theta_k)\big)^2 A^i + \Lambda_N A^i, \tag{3.3}$$

where A^i is the vector $(a_1^i, \dots, a_N^i)$ and the matrix Λ_N is the infinitesimal generator of the jump process with parameter β. The system of differential equations (3.2) is equipped with the initial condition $a_r^i(0) = a_{r,\lambda_i,\mu_i}$ with a_{r,λ_i,μ_i} from (3.1).

The following theorem holds.

Theorem 1. *For any almost periodic polynomial initial condition in $SE(2, N, K)$, the integration of the diffusion equation reduces to solving a finite set of independent linear ordinary differential equations of dimension N. Any continuous initial condition over a compact subset of $SE(2, N)$ can be uniformly approximated by such a polynomial.*

Differential equations (3.2) over $\mathbb{C}^N$ are not hard to tract numerically. They have an elliptic right hand term, and the Crank-Nicolson method (discussed in the next section) is recommended.

In fact, $SE(2, N, K)$ is the space of a unitary representation of $SE(2, N)$ which is not irreducible but splits into the direct sum of irreducible representations:

$$SE(2, N, K) = \bigoplus_{\omega \in K} SE(2, N, \{\omega\}).$$

This fact suggests that we can use our knowledge of the dual $\widehat{SE(2, N)}$ to reduce the computations. Actually, it is easy to check that for $\widetilde{\omega}, \omega \in K$ such that $\widetilde{\omega} = R_r\omega$, if we call $\widetilde{A}$ and A the corresponding solutions of Equation (3.3) in $SE(2, N, \{\widetilde{\omega}\})$ and $SE(2, N, \{\omega\})$, respectively, we get:

$$\begin{aligned}
\frac{dA}{dt} &= -\frac{1}{2}\mathrm{diag}_k\big(\lambda_i \cos(\theta_k) + \mu_i \sin(\theta_k)\big)^2 A + \Lambda_N A, \\
\frac{dS^r\widetilde{A}}{dt} &= -\frac{1}{2}\mathrm{diag}_k\big(\lambda_i \cos(\theta_k) + \mu_i \sin(\theta_k)\big)^2 S^r\widetilde{A} + \Lambda_N S^r\widetilde{A}.
\end{aligned}$$

So that it is not necessary to compute all the resolvents relative to each unitary irreducible representation. It is enough to do it for those corresponding to $\omega \in \widehat{SE(2, N)}$.

Theorem 2. *In theorem 1, if some points of K can be deduced one from the other by elementary rotations R_r then it is enough to compute the resolvents corresponding to a single among these points.*

This method could be very efficient in a general setting. The last considerations show that it is of numerical interest to put in K as much as possible points in the same orbits under the elementary rotations.

In our vision problem, the initial conditions are certainly very far from being almost periodic. Hence we preferred a more direct method, which is however closely related with this one. This is explained in the next section.

4. Final algorithm

In fact, images being given under the guise of a square table of real values (the grey levels), we have chosen to deal with periodic images over a basic square, and to discretize with respect to the naturally discrete (x, y) variables. We take a mesh of $M_x \times M_y$ points on the (x, y)-plane, and the number of angles is N.

Remark 3. *In practice, in all the results we show,* $M_x = M_y = M = 256$*, and the number of angles* $N \approx 30$*.* ***We don't see any significant improvement for larger*** N*.*

Therefore, a function $\psi(x, y, \theta)$ over $SE(2, N)$ is approximated by a $M^2 \times N$ table $(\psi^p_{k,l})$, $p = 1, \dots, N$, $k, l = 1, \dots, M$. Hence, without loss of generality, we set for the discretization steps $\Delta x = \Delta y = \sqrt{M}$ and the mesh points are $x_k = \frac{k-1}{\sqrt{M}}$, $y_l = \frac{l-1}{\sqrt{M}}$. In this section, due to the periodicity, the upper index takes natural values modulo N and the lower indices take natural values modulo M.

Remind that the semi-discrete diffusion equation over $SE(2, N)$ is (2.8). For numerical solution of this equation we replace the differential operators $\frac{\partial}{\partial x}, \frac{\partial}{\partial y}$ by the discrete operators D_x, D_y, which act on $\mathbb{C}^{M^2}$:

$$D_x(\psi^p_{k,l}) = \frac{\psi^p_{k+1,l} - \psi^p_{k-1,l}}{x_{k+1} - x_{k-1}} = \frac{\sqrt{M}}{2}\big(\psi^p_{k+1,l} - \psi^p_{k-1,l}\big),$$
$$D_y(\psi^p_{k,l}) = \frac{\psi^p_{k,l+1} - \psi^p_{k,l-1}}{y_{l+1} - y_{l-1}} = \frac{\sqrt{M}}{2}\big(\psi^p_{k,l+1} - \psi^p_{k,l-1}\big).$$

Then we get the diffusion equation with totally discretized (i.e., with discretized space and angle variables) operator D, which acts on $\mathbb{C}^N \otimes \mathbb{C}^{M^2} \simeq \mathbb{C}^{N \cdot M^2}$:

$$\frac{d\psi^p_{k,l}}{dt} = \frac{1}{2} D(\psi^p_{k,l}), \quad \text{where} \tag{4.1}$$
$$D(\psi^p_{k,l}) = \big(\cos(e_p)D_x + \sin(e_p)D_y\big)^2(\psi^p_{k,l}) + \beta(\psi^{p-1}_{k,l} - 2\psi^p_{k,l} + \psi^{p+1}_{k,l}).$$

The initial condition for (4.1) is the discrete analog of the function $\overline{f}(x, y, \theta)$ obtained after the lift of the original image $f(x, y)$.

Remark 4. *For* $M = 256$*,* $N = 30$ (4.1) *is a fully coupled linear differential equation in* $\mathbb{R}^K$*,* $K = 1,996,080$*. Applying an implicit or semi-implicit finite difference scheme, one need to solve a system of* $K^2 \approx 3.6 \times 10^{12}$ *linear algebraic equations.*

As previously, it is natural to apply the Fourier transform over the abelian group $(\mathbb{Z}/M\mathbb{Z})^2$, which can be computed **exactly** by the standard FFT (Fast Fourier Transform) algorithm. Let us denote by $\widehat{\psi}$ the Fourier transform of ψ:

$$\widehat{\psi}^p_{k,l} = \frac{1}{M} \sum_{r,s=1}^{M} \psi^p_{r,s} \exp\left(-2\pi i \left(\frac{(k-1)(r-1)}{M} + \frac{(l-1)(s-1)}{M}\right)\right).$$

A straightforward computation shows that

$$\widehat{D_x(\psi^p_{k,l})} = i\sqrt{M} \sin\left(2\pi \frac{k-1}{M}\right) \widehat{\psi}^p_{k,l}, \quad \widehat{D_y(\psi^p_{k,l})} = i\sqrt{M} \sin\left(2\pi \frac{l-1}{M}\right) \widehat{\psi}^p_{k,l},$$

and the Fourier transform maps the operator $\cos(e_p)D_x + \sin(e_p)D_y$ to the multiplication operator $\widehat{\psi}^p_{k,l} \to i\sqrt{M}\, a^p_{k,l} \widehat{\psi}^p_{k,l}$, where

$$a^p_{k,l} = \cos(e_p) \sin\left(2\pi \frac{k-1}{M}\right) + \sin(e_p) \sin\left(2\pi \frac{l-1}{M}\right).$$

Hence, the diffusion equation (4.1) is mapped to the following completely decoupled system of M^2 linear differential equations over $\mathbb{C}^N$:

$$\frac{d\widehat{\psi}_{k,l}}{dt} = A_{k,l}\,\widehat{\psi}_{k,l}, \quad \widehat{\psi}_{k,l} = (\widehat{\psi}^1_{k,l}, \dots, \widehat{\psi}^N_{k,l}), \tag{4.2}$$

where $A_{k,l} = \frac{1}{2}\big(\Lambda_N - M\mathrm{diag}_p(a^p_{k,l})^2\big)$, and Λ_N is an almost tridiagonal $N \times N$ matrix: due to periodicity in p, Λ_N contains two extra non-zero elements in the right-up and left-low corners.

Therefore the solution of (4.2) is

$$\widehat{\psi}_{k,l}(t) = e^{tA_{k,l}}\widehat{\psi}_{k,l}(0), \tag{4.3}$$

where the initial function $\widehat{\psi}_{k,l}(0)$ is known. Finally, the solution of (4.1) is the inverse Fourier transform over $(\mathbb{Z}/M\mathbb{Z})^2$ of $\widehat{\psi}^p_{k,l}(t)$, obtained using the inverse FFT.

Theorem 3. *The solution of Equation* (4.1) *can be computed* ***exactly*** *by solving in parallel M^2 linear differential equations in dimension N.*

For instance, for $M = 256$ and $N = 30$, this is solving 65536 linear differential equations in dimension 30.

Remark 5. *1. The complexity of the FFT used twice in our algorithm (including the inverse transform) is negligible in front of the complexity of the numerical integration of the decoupled linear differential equations.*

2. The discretized diffusion (4.1) *can be numerically integrated with the semi-explicit Crank-Nicolson scheme. The convergence of this scheme for the considered class of equations and some estimations are well known; see e.g.* [24, chapter 5]. *Note that the matrices $A_{k,l}$ are tridiagonal plus two terms in the right-up and left-low corners (coming from Λ_N due to periodicity). An effective algorithm for solving such linear system is suggested in* [1].

3. Formula (4.3) *for solutions of the linear differential equations* (4.2) *has an obvious advantage. Once M, N and α (or, equivalently, β) are fixed, the matrices $A_{k,l}$* ***are universal****, and therefore their exponentials can be computed once for all. Moreover, using a time step τ and the formula $e^{n\tau A_{k,l}} = \big(e^{\tau A_{k,l}}\big)^n$, it is enough to compute only the exponential $e^{\tau A_{k,l}}$.*

4. In fact, it is not necessary to compute M^2 exponentials of matrices: it is enough to compute them at the points k, l that fall in the dual space $\widehat{SE(2,N)}$. This is much less. For large N, is number is of order M in place of M^2. Here, the structure of $SE(2,N)$ is crucial, and specially formula (2.10).

5. Preservation of non-corrupted parts

It has to be noticed that:

- The treatment of images up to now is essentially global.
- It is not necessary to know where the image is corrupted.

Presumably, the visual cortex V1 is also able in some cases to detect that the image is corrupted at some place, and to take this a-priori knowledge into account. We tried to investigate a method that would improve on our algorithm in this direction. We suggest (essentially heuristically) the following procedure.

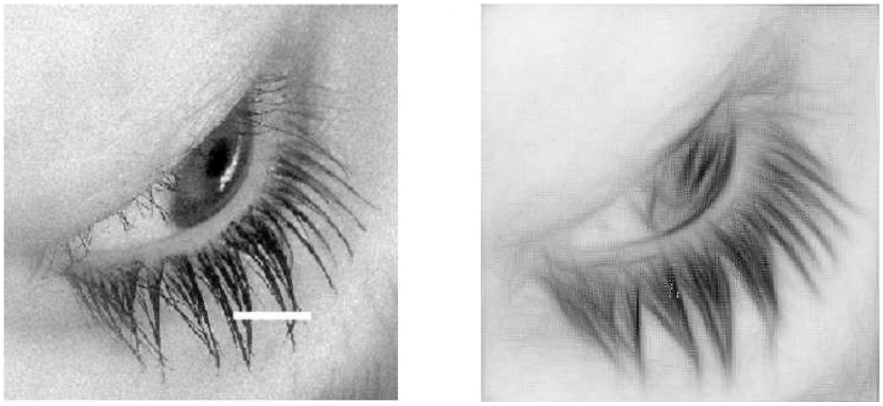

FIGURE 1. The initial corrupted image (left) and the image reconstructed via diffusion (right).

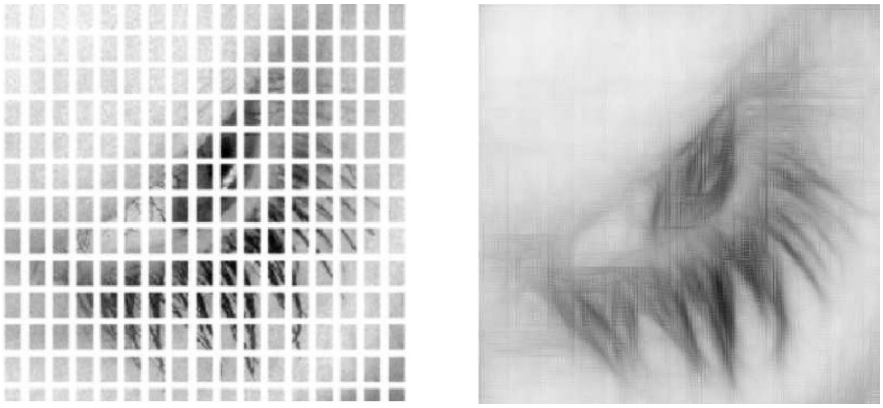

FIGURE 2. The initial corrupted image (left) and the image reconstructed via diffusion (right).

5.1. **Motivation.** One natural idea would be to iterate the following steps:

- Lift the plane image to $PT\mathbb{R}^2$.
- Integrate the diffusion equation for some fixed small τ.
- Project the solution down to the plane.
- Restore the non-corrupted part of the initial image.

In practice, this idea does not work at all. The main reason is that the diffusion acts on both the corrupted and the non-corrupted parts, and there is not good coincidence at the frontier after the restoration.

All variations of the previous idea, at the level of the plane image do not provide acceptable results. From what we conclude that it is necessary to proceed the restoration of the the non-corrupted part at the level of the lifted image, i.e., on the bundle $PT\mathbb{R}^2$.

5.2. **Description of the "preservation" procedure.** Assume that points (x, y) of the image under reconstruction are separated into the set G of "good" (non-corrupted) and the set B of "bad" (corrupted) points; $f(x, y) = 0$ for all $(x, y) \in B$ and $f(x, y) > 0$ for all $(x, y) \in G$. We would like to preserve points of the set G from the effect of diffusion, while on the set B the diffusion should be proceeded.

The general idea of the "preservation" procedure is to "mix" the solution $\psi(x, y, \theta, t)$ of the diffusion equation with the initial function $\psi(x, y, \theta, 0) = \overline{f}(x, y, \theta)$ at each point $(x, y) \in G$. The "mixing" is fulfilled many times during the integration of our equation.

Namely, split the segment $[0, T]$ into n small intervals with the mesh points $t_i = i\tau$, $\tau = T/n$, $i = 0, 1, \ldots, n$, and proceed the integration of our equation on each $[t_i, t_{i+1}]$ with the initial condition

$$\psi\big|_{t=t_i} = \begin{cases} \psi(x, y, \theta, t_i), \text{ if } (x, y) \in B, \\ \sigma(x, y, t_i)\, \psi(x, y, \theta, t_i), \text{ if } (x, y) \in G, \end{cases}$$

where the function $\psi(x, y, \theta, t_i)$ is computed after integration on the previous interval, and the factor $\sigma(x, y, t_i)$ is defined by

$$\sigma(x, y, t_i) = \frac{\epsilon h(x, y, 0) + (1 - \epsilon) h(x, y, t_i)}{h(x, y, t_i)}, \qquad h(x, y, t) = \max_{\theta} \psi(x, y, \theta, t),$$

where $0 \le \epsilon \le 1$. After that we obtain the function $\psi(x, y, \theta, t_{i+1})$ and repeat the procedure on the next interval.

Note that this procedure essentially depends on two parameters that can be chosen experimentally: the natural number n (number of treatments) and the coefficient ϵ, which defines the strength of each treatment.

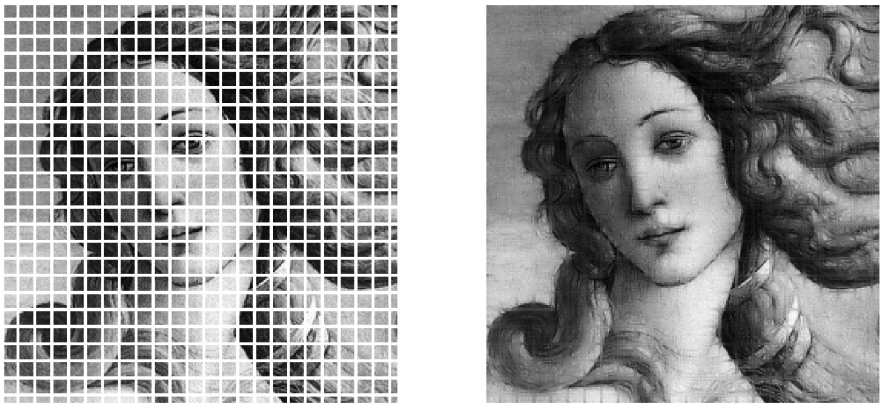

FIGURE 3. The initial corrupted image (left, 32% damaged) and the image reconstructed via diffusion with the "preservation" procedure (right).

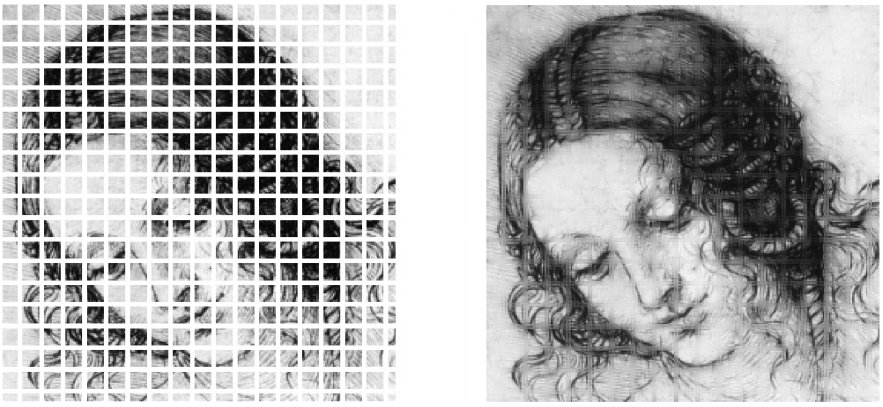

FIGURE 4. The initial corrupted image (left, 37% damaged) and the image reconstructed via diffusion with the "preservation" procedure (right).

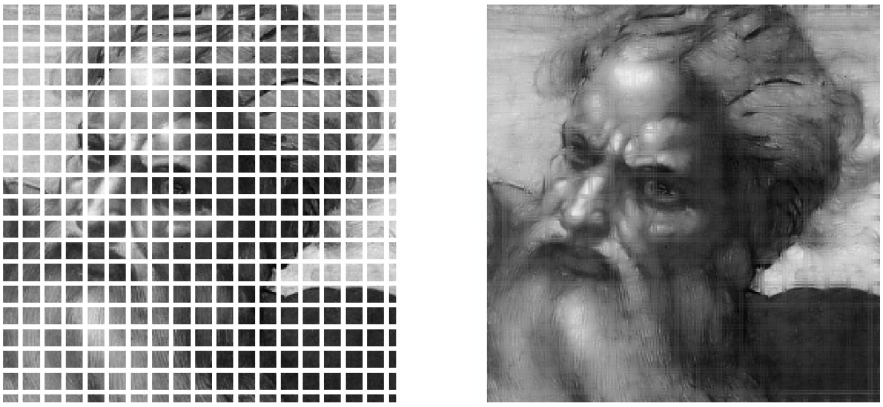

FIGURE 5. The initial corrupted image (left, 37% damaged) and the image reconstructed via diffusion with the "preservation" procedure (right).

6. Appendix

In this appendix, we collect shortly a few results needed for the understanding of the paper.

6.1. **The Generalized Fourier Transform (GFT).** Given a locally compact unimodular topological group G of Type I[5], the dual $\widehat{G}$ is the set of (strongly) continuous complex unitary irreducible representations $(\chi_{\widehat{g}}, H_{\widehat{g}})$ of G. For $\widehat{g} \in \widehat{G}$, $\chi_{\widehat{g}} \colon G \to U(H_{\widehat{g}})$, the unitary group of the complex Hilbert space $H_{\widehat{g}}$. The space of complex L^2 functions over G with respect to the Haar measure is denoted by

[5]We do not say what type I means. We just need here to know that both $SE(2)$ and $SE(2,N)$ are type I. For instance, any connected semi-simple or nilpotent group is type I.

$L^2(g, dg)$. The generalized Fourier transform (GFT) of $f \in L^2(g, dg)$ is defined by[6]:

$$\widehat{f}(\widehat{g}) = \int_G f(g)\chi_{\widehat{g}}(g^{-1})\, dg. \tag{6.1}$$

The operator $\widehat{f}(\widehat{g})$ is Hilbert-Schmidt over $H_{\widehat{g}}$ and there is a measure $d\widehat{g}$ over $\widehat{G}$, called the Plancherel measure, such that the GFT is an isometry to $L^2(\widehat{g}, d\widehat{g})$, where the space $L^2(\widehat{g}, d\widehat{g})$ is the continuous Hilbert sum of the spaces of Hilbert-Schmidt operators over the spaces $H_{\widehat{g}}$, with respect to Plancherel's measure. As a consequence, we have the inversion formula:

$$f(g) = \int_{\widehat{G}} \widehat{f}(\widehat{g})\chi_{\widehat{g}}(g)\, d\widehat{g}. \tag{6.2}$$

The GFT is a natural extension of the ordinary Fourier transform over abelian groups and it has all the corresponding properties, such as: mapping convolution to product, etc. (see [2]).

As in the case of the usual heat equation over $\mathbb{R}^n$, we use it to solve our heat equations over the groups $SE(2)$ and $SE(2, N)$.

6.2. **Bohr Compactification and Almost Periodic Functions.** The Bohr compactification of a topological group G is the universal object $(G^\flat, \widetilde{\sigma})$ in the category of diagrams:

$$\sigma\colon G \to H,$$

where σ is a continuous homomorphism from G to a compact group H. If the mapping $\widetilde{\sigma}\colon G \to G^\flat$ is injective, G is called maximally almost periodic (MAP).

The set $AP(G)$ of almost periodic functions over G is the pull back by $\widetilde{\sigma}$ of the set of continuous functions over $G^\flat$.

The group G is MAP iff the continuous unitary finite dimensional representations of G separate the points. A connected locally compact group is MAP iff it is the direct product of a compact group by $\mathbb{R}^n$. For instance, $SE(2, N)$ is MAP, while $SE(2)$ is not.

A continuous function $f \in AP(G)$ iff its right (or left) translated form a relatively compact subset of $E(G)$, the set of bounded continuous functions over G, iff it is a uniform limit of coefficients of unitary irreducible representations of G. If G is MAP, $AP(G)$ is dense in the space of continuous functions over G, in the topology of uniform convergence over compact sets.

For duality over MAP groups, see [8] and the book [20]. For introduction to almost periodic functions, see the original paper [36] and the nice exposition [16].

6.3. **Proof that expressions** (2.10) **and** (2.12) **are identical.** In this section, all integer indices take values between 1 and N, and addition is always modulo N.

[6]As usual, the integral below is well defined for $f \in L^1(G, dg)$ only, but is extended by continuity.

Set $M_{\lambda,\nu}(t) = e^{\widetilde{A}_{\lambda,\nu}t}$, where the matrix $\widetilde{A}_{\lambda,\nu}$ is defined in (2.9). Then we need to establish the identity of the two expressions:

$$D^1_t(z,e_r) = \int\limits_{\widehat{SE(2,N)}} \mathrm{trace}\Big(M_{\lambda,\nu}(t)\cdot \mathrm{diag}_k\Big(e^{i\langle V_{\lambda,\nu},R_k z\rangle}\Big)S^r\Big)\lambda d\lambda d\nu,$$

$$D^2_t(z,e_r) = \int\limits_{\mathbb{R}^2} \big(M_{\lambda,\nu}(t)\delta_N\big)_r\, e^{i\langle V_{\lambda,\nu},z\rangle}\lambda d\lambda d\nu.$$

Set

$$M^r_{\lambda,\nu}(t) = e^{\widetilde{A}^r_{\lambda,\nu}t}, \quad \widetilde{A}^r_{\lambda,\nu} = \Lambda_N - \mathrm{diag}_k\big(\lambda^2\cos^2(e_{k+r}-\nu)\big).$$

The following fact is crucial:

$$S^{-r}M_{\lambda,\nu}(t)S^r = M^r_{\lambda,\nu}(t), \tag{6.3}$$

where S is the shift matrix over $\mathbb{C}^N$ (i.e., $Se_k = e_{k+1}$ for $k = 1,\dots,N-1$, and $Se_N = e_1$). The equality (6.3) follows from $S^{-r}\widetilde{A}^r_{\lambda,\nu}S^r = \widetilde{A}_{\lambda,\nu}$, a consequence of $S^{-r}\Lambda_N S^r = \Lambda_N$ and of the general relation

$$(S^{-r}BS^r)_{n,m} = B_{n-r,m-r}, \tag{6.4}$$

which holds true for any $N\times N$ matrix B.

An immediate computation shows that

$$D^1_t(z,e_r) = \int\limits_{\widehat{SE(2,N)}} \sum_n \Big(M_{\lambda,\nu}(t)\cdot \mathrm{diag}_k\Big(e^{i\langle V_{\lambda,\nu},R_k z\rangle}\Big)\Big)_{n+r,n}\lambda d\lambda d\nu = \tag{6.5}$$

$$\int\limits_{\widehat{SE(2,N)}} \sum_n \big(M_{\lambda,\nu}(t)\big)_{n+r,n} e^{i\langle V_{\lambda,\nu},R_n z\rangle}\lambda d\lambda d\nu.$$

On the other hand, using the relations (6.3) and (6.4), we have:

$$D^2_t(z,e_r) = \int\limits_{\mathbb{R}^2} \big(M_{\lambda,\nu}(t)\delta_N\big)_r\, e^{i\langle V_{\lambda,\nu},z\rangle}\lambda d\lambda d\nu = \int\limits_{\mathbb{R}^2} \big(M_{\lambda,\nu}(t)\big)_{r,N}\, e^{i\langle V_{\lambda,\nu},z\rangle}\lambda d\lambda d\nu =$$

$$\int\limits_{\widehat{SE(2,N)}} \sum_n \big(M^n_{\lambda,\nu}(t)\big)_{r,N}\, e^{i\langle V_{\lambda,\nu-e_n},z\rangle}\lambda d\lambda d\nu =$$

$$\int\limits_{\widehat{SE(2,N)}} \sum_n \big(S^{-n}M_{\lambda,\nu}(t)S^n\big)_{r,N}\, e^{i\langle V_{\lambda,\nu},R_{-n}z\rangle}\lambda d\lambda d\nu =$$

$$\int\limits_{\widehat{SE(2,N)}} \sum_n \big(M_{\lambda,\nu}(t)\big)_{r-n,N-n}\, e^{i\langle V_{\lambda,\nu},R_{-n}z\rangle}\lambda d\lambda d\nu.$$

Finally, changing n for $-n$ and observing that $N+n = n$, we get the following expression:

$$D^2_t(z,e_r) = \int\limits_{\widehat{SE(2,N)}} \sum_n \big(M_{\lambda,\nu}(t)\big)_{n+r,n}\, e^{i\langle V_{\lambda,\nu},R_n z\rangle}\lambda d\lambda d\nu,$$

which is exactly (6.5).

Acknowledgement 1. *The authors thank Prof. Eric Busvelle for his help.*

Acknowledgement 2. *This research has been supported by the Europen Research Council, ERC StG 2009 "GeCoMethods" (contract 239748), by the ANR "GCM" (programme blanc NT09-504490), and by the DIGITEO project CONGEO.*

References

[1] A.A. Abramov, V.B. Andreev, On the application of the method of successive substitution to the determination of periodic solutions of differential and differences equations, Zh. Vychisl. Mat. Mat. Fiz., 3.2, 1963, pp. 377–381.

[2] A. Agrachev, U. Boscain, J.-P. Gauthier, F. Rossi, The intrinsic hypoelliptic Laplacian and its heat kernel on unimodular Lie groups, J. Funct. Anal., 256 (2009), pp. 2621–2655.

[3] A.A. Agrachev, Yu. L. Sachkov, Control Theory from the Geometric Viewpoint, Encyclopedia of Mathematical Sciences, v. 87, Springer, 2004.

[4] N.U. Ahmed, T.E. Dabbous, Nonlinear Filtering of systems governed by ITO Differential Equations with Jump Parameters, Journal of Mathematical Analysis and Applications, 115 (1986), pp. 76–92.

[5] U. Boscain, G. Charlot, F. Rossi, Existence of planar curves minimizing length and curvature, Journal of Mathematical Sciences, to appear, arXiv:0906.5290.

[6] U. Boscain, J. Duplaix, J.P. Gauthier, F. Rossi, Anthropomorphic image reconstruction via hypoelliptic diffusion. SIAM J. CONTROL OPTIM., Vol. 50, no. 3 (2012), pp. 1309–1336.

[7] F. Cao, Y. Gousseau, S. Masnou, P. Pérez, Geometrically guided exemplar-based inpainting, submitted.

[8] H. Chu, Compactification and duality of topological groups, Trans. Am. Math. Soc. 123, 1966, pp. 310–324.

[9] G.S. Chirikjian, A.B. Kyatkin, Engineering applications of noncommutative harmonic analysis, CRC Press, Boca Raton, FL, 2001.

[10] G. Citti, A. Sarti, A cortical based model of perceptual completion in the roto-translation space, J. Math. Imaging Vision 24 (2006), no. 3, pp. 307–326.

[11] C. Corduneanu, N. Gheorgiu, V. Barbu, Almost Periodic Functions, second edition,Chelsea Publishing Company, 1989.

[12] J. Damon, Generic structure of two-dimensional images under Gaussian blurring, SIAM J. Appl. Math., Vol. 59, No. 1 (1998), pp. 97–138.

[13] R. Duits, M. van Almsick, The explicit solutions of linear left-invariant second order stochastic evolution equations on the 2D Euclidean motion group. Quart. Appl. Math. 66 (2008), pp. 27–67.

[14] R. Duits, E.M. Franken, Left-invariant parabolic evolutions on SE(2) and contour enhancement via invertible orientation scores, Part I: Linear Left-Invariant Diffusion Equations on $SE(2)$ Quart. Appl. Math., 68 (2010), pp. 293–331.

[15] R. Duits, E.M. Franken, Left-invariant parabolic evolutions on SE(2) and contour enhancement via invertible orientation scores, Part II: nonlinear left-invariant diffusions on invertible orientation scores Quart. Appl. Math., 68 (2010), pp. 255–292.

[16] J. Dixmier, Les C^*-algèbres et leurs représentations, second edition, Gauthier-Villars, Paris, 1969.

[17] E.M. Franken, Enhancement of Crossing Elongated Structures in Images. Ph. D. Thesis, Eindhoven University of Technology, 2008, Eindhoven, http://alexandria.tue.nl/extra2/200910002.pdf

[18] E.M. Franken, R. Duits, Crossing-Preserving Coherence-Enhancing Diffusion on Invertible Orientation Scores., IJCV, 85 (3), 2009, pp. 253–278.

[19] M. Gromov, Carnot-Caratheodory spaces seen from within, in Sub-Riemannian geometry, Progr. Math., vol. 144, Birkhäuser, Basel, 1996, pp. 79–323.

[20] H. Heyer, Dualität über Lokal Kompakter Gruppen, Springer Berlin, 1970.

[21] R.K. Hladky, S.D. Pauls, Minimal Surfaces in the Roto-Translation Group with Applications to a Neuro-Biological Image Completion Model, J. Math. Imaging Vis. 36 (2010), pp. 1–27.

[22] L. Hörmander, Hypoelliptic Second Order Differential Equations, Acta Math., 119 (1967), pp. 147–171.

[23] M. Langer, Computational Perception, Lecture Notes, Centre for Intelligent Machines, 2008, http://www.cim.mcgill.ca/∼langer/646.html
[24] G.I. Marchuk, Methods of Numerical Mathematics. Application of Mathematics, 2. Springer-Verlag, 1982.
[25] D. Marr, E. Hildreth, Theory of Edge Detection, Proceedings of the Royal Society of London. Series B, Biological Sciences, Vol. 207, No. 1167. (Feb. 29, 1980), pp. 187–217.
[26] I. Moiseev, Yu. L. Sachkov, Maxwell strata in sub-Riemannian problem on the group of motions of a plane, ESAIM: COCV 16, no. 2 (2010), pp. 380–399.
[27] D. Mumford, Elastica and computer vision. Algebraic Geometry and Its Applications. Springer-Verlag, 1994, pp. 491–506.
[28] L. Peichl, H. Wässle, Size, scatter and coverage of ganglion cell receptive eld centres in the cat retina, J. Physiol., Vol. 291, 1979, pp. 117–41.
[29] J. Petitot, Vers une Neuro-géomètrie. Fibrations corticales, structures de contact et contours subjectifs modaux, Math. Inform. Sci. Humaines, no. 145 (1999), pp. 5–101.
[30] J. Petitot, Neurogéomètrie de la vision – Modèles mathématiques et physiques des architectures fonctionnelles, Les Éditions de l' École Polythecnique, 2008.
[31] Yu. L. Sachkov, Conjugate and cut time in the sub-Riemannian problem on the group of motions of a plane, ESAIM: COCV 16 (2010), pp. 1018–1039.
[32] Yu. L. Sachkov, Cut locus and optimal synthesis in the sub-Riemannian problem on the group of motions of a plane, ESAIM: COCV 17 (2011), pp. 293–321.
[33] G. Sanguinetti, G. Citti, A. Sarti, Image completion using a diffusion driven mean curvature flowin a sub-Riemannian space, in: Int. Conf. on Computer Vision Theory and Applications (VISAPP'08), FUNCHAL, 2008, pp. 22–25.
[34] N.Y. Vilenkin, Special functions and the theory of group representations, American Mathematical Soc., 1968.
[35] G. Warner, Harmonic Analysis on Semi-Simple Groups, Vols. 1 and 2, Springer-Verlag, 1972.
[36] A. Weil, L'intégration dans les groupes topologiques et ses applications. Publications de L'institute de Mathématique de L'université de Strasbourg. Paris, Hermann, 1953.